A Ku-band magnetically insulated transmission line oscillator with overmoded slow-wave-structure*

Tao Jiang(江涛), Jun-Tao He(贺军涛), Jian-De Zhang(张建德)†,
Zhi-Qiang Li(李志强), and Jun-Pu Ling(令钧溥)

College of Optoelectric Science and Engineering, National University of Defense Technology, Changsha 410073, *China*

(Received 11 July 2016; revised manuscript received 8 August 2016; published online 25 October 2016)

In order to enhance the power capacity, an improved Ku-band magnetically insulated transmission line oscillator (MILO) with overmoded slow-wave-structure (SWS) is proposed and investigated numerically and experimentally. The analysis of the dispersion relationship and the resonant curve of the cold test indicate that the device can operate at the near π mode of the TM01 mode, which is useful for mode selection and control. In the particle simulation, the improved Ku-band MILO generates a microwave with a power of 1.5 GW and a frequency of 12.3 GHz under an input voltage of 480 kV and input current of 42 kA. Finally, experimental investigation of the improved Ku-band MILO is carried out. A high-power microwave (HPM) with an average power of 800 MW, a frequency of 12.35 GHz, and pulse width of 35 ns is generated under a diode voltage of 500 kV and beam current of 43 kA. The consistency between the experimental and simulated far-field radiation pattern confirms that the operating mode of the improved Ku-band MILO is well controlled in π mode of the TM01 mode.

Keywords: Ku-band, MILO, HPM, overmoded SWS, mode selection, particle simulation, experimental investigation

PACS: 52.59.–f, 52.65.Rr, 52.70.Gw **DOI:** 10.1088/1674-1056/25/12/125202

1. Introduction

The magnetically insulated transmission line oscillator (MILO) is a kind of cross-field device, which can produce a gigawatt-class high-power microwave (HPM) without using any external applied magnetic field.[1,2] The intrinsic self-magnetic insulation property of MILO makes it more compact and lightweight than any other HPM sources such as relativistic magnetron (RM), relativistic backward wave oscillator (RBWO), and relativistic klystron amplifier (RKA).[1,2] Thus, as an attractive source, the MILO has been extensively studied in both theory and experiment since it was invented in 1987.[1–20] At present, an HPM output of over 1 GW can be stably generated in the MILOs of L, S, and C bands,[3–15] In particular, Fan *et al.* designed the L-band MILO that can generate 3.2 GW microwave output at 1.2 GHz, which is the top level in the world according to the reported literature.[15]

In order to enhance the Pf^2 factor, in which P and f are the output power and frequency of the microwave, respectively, the enhancement of operation frequency of the HPM resource is a development direction. In addition, due to the wide applications in digital communication field of the Ku-band microwave, the Ku-band HPM source has become one of the major hotspots in the field of HPM research.[19–27]

However, with the enhancement of the operation frequency, the size of the device is smaller. The power capacity becomes one restriction of the high frequency band HPM resources. In 2013, Wen *et al.* first conducted the research of Ku-band MILO.[19,20] But the device only produced a microwave with a power of 89 MW and pulse width of 16 ns in the experiment due to the small power capacity of the device and the erosion of the load area.[19,20] We also studied the Ku-band MILO and carried out the preliminary experiment in a traditional Ku-band MILO device, but the device only generated a microwave with a power of 150 MW and pulse width of 17 ns, which are inconsistent with the simulation results.[27] Analysis of the experimental results shows that the radio-frequency (RF) breakdown on the slow-wave-structure (SWS) is the main cause for the low microwave output power and short pulse width. Usually, as the operating frequency increases, to achieve high power capacity, overmoded SWSs with large diameters are employed in HPM generators.[23,28,29] In 2014, Zhang *et al.* designed a Ku-band Cerenkov generator and conducted the experimental investigation.[23–25] The power capacity of the device is enhanced by adopting overmoded SWS. Ultimately, the device achieved a 1-GW HPM output.[23]

In this paper, an improved Ku-band MILO with overmoded SWS is designed and investigated numerically and experimentally.

*Project supported partly by the National Natural Science Foundation of China (Grant No. 61171021).
†Corresponding author. E-mail: jdzhang12@yahoo.com
© 2016 Chinese Physical Society and IOP Publishing Ltd

2. Model description of the improved Ku-band MILO

The schematic of the improved Ku-band MILO proposed in this paper is shown in Fig. 1. As can be seen from Fig. 1, the MILO primarily consists of six parts, which are the SWS, choke cavity, double-cavities extractor, ladder cathode, limited load, and coaxial output waveguide. Among them, a choke cavity is adopted to prevent the microwave from propagating into the pulse power source and a double-cavities extractor is used to enhance the microwave extracting efficiency. Besides, it is confirmed that the limited load structure is able to eliminate the electrode erosion of the load due to the large load anode–cathode gap and small energy deposition density in the first Ku-band MILO designed by us. Additionally, the ladder cathode is adopted to replace the traditional uniform cathode, which is beneficial to the improvement of the conversion efficiency.[30–32] The edges of all the vanes used to constitute the SWS cavities are rounded with a radius of 1 mm to reduce the RF field of the SWS surface, which is conducible to improving the power capacity and minimizing the risk of rf breakdown.

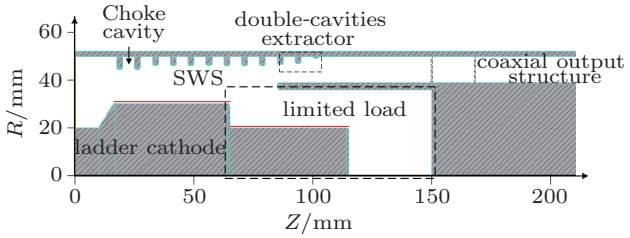


Fig. 1. (color online) The schematic diagram of the improved Ku-band MILO.

In order to enhance the power capacity, the improved Ku-band MILO adopts overmoded SWS. Compared with that of the first Ku-band MILO designed by us, the overall size of the improved one is increased significantly, specifically, the cathode–anode gap is increased from 12 mm to 16 mm. Through this improvement, the power capacity of the device will be enhanced significantly without a doubt. However, mode competition occurs more easily when using overmoded SWS because more modes can exist in the overmoded SWS, which is the biggest difficulty in designing the overmoded SWS. So we should be more careful in mode selection and control when the overmoded SWS is designed.

3. Mode selection and control

The operating frequency of the MILO is determined mainly by the dimension parameters of the main SWS. Normally, the MILO operates at the near π mode of the TM01 mode due to its great coupling impedance.[1,2] Therefore, when designing the overmoded SWS, the operation point must be selected near the π mode of the TM01 mode. The analysis of the dispersion relationship is conducible to designing the high frequency structure.

The profile of the main SWS is shown in Fig. 2 and the dimensions of the parameters are presented in Table 1. Compared with that of the normal SWS, the AK gap of the Ku-band MILO is increased significantly to enhance the power capacity. The AK gap of the first Ku-band MILO designed by us[27] is 12 mm and the AK gap of the Ku-band MILO proposed in this paper is increased to 16 mm (r_{ai}–r_c). Accordingly, the period of SWS is increased from 6.5 mm to 7.5 mm (L). Therefore, the power capacity of the Ku-band MILO will be enhanced significantly.

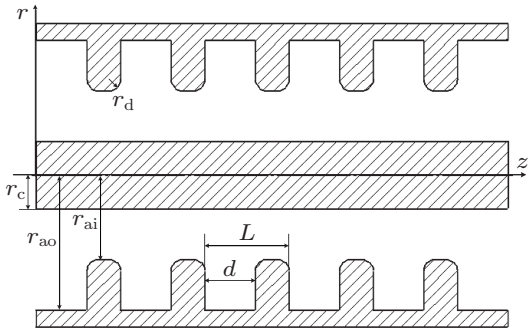


Fig. 2. Profile of the main SWS.

Table 1. Sizes of the parameters of the main SWS.

Parameter	r_{ao}/mm	r_{ai}/mm	R_c/mm	L/mm	d/mm	R_d/mm
Dimension	50	46	30	7.5	3	1

The dispersion curves of TM01 and TM02 modes of the SWS are calculated by a high frequency electromagnetic simulation program (HFSS), and shown in Fig. 3 where the light line and the beam line with energy of 500 keV are also plotted.

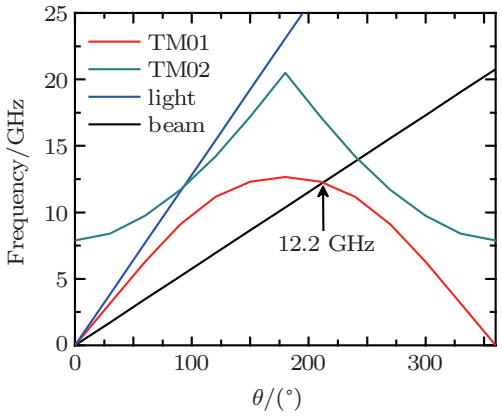


Fig. 3. (color online) Dispersion curves of the SWS and the beam line.

It should be noted that the dispersion curves of TM01 mode and TM02 mode are not separated from each other by a forbidden frequency band, which is not the same as the scenarios of the MILOs in low frequency bands. This shows that the SWS is overmoded, which is due to the large cathode–anode gap of the improved Ku-band MILO. The adoption of

overmoded SWS is to enhance the power capacity. Multimode may be excited and the mode competition between adjacent modes may emerge in the overmoded device.[28] The electron beam line intersects with the TM01 mode at a frequency of 12.2 GHz, which is around the π mode point of 12.7 GHz. This indicates that the device can operate at the near π mode of the TM01 mode, which is useful for mode selection and control.

In order to further confirm the operating mode, a numerical cold test method is used to investigate the resonant characteristic of the designed electrodynamic structure by exciting one SWS gap with an impulse signal. In the simulation, the impulse signal is loaded on the surface of the fourth main SWS cavity. The resonant curve is shown in Fig. 4. As can be seen from the figure, the most easily excited resonant frequency is 12.4 GHz, which is near to the π mode point of the TM01 mode and the other resonant frequencies are suppressed well in the device. The electric field distribution of the mode at 12.4 GHz is detected, and the results are as shown in Fig. 5. It can be concluded that this mode of 12.4 GHz is the π mode of the TM01 mode. It is in good agreement with the dispersion curves discussed in Fig. 3. The near π mode of the TM01 mode will be chosen as the operating mode, which is helpful in improving the power conversion efficiency and useful for mode selection and control.[23,32]

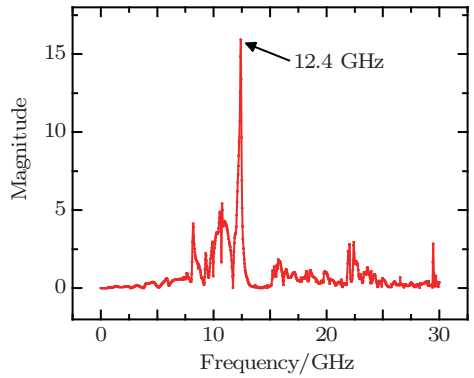


Fig. 4. (color online) Resonant curve in cold test.

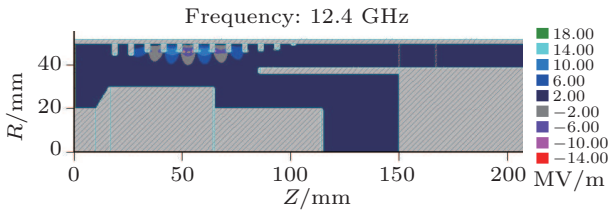


Fig. 5. (color online) Electric field distribution of the mode at 12.4 GHz.

4. Simulation results and analysis

Particle simulations are conducted with the PIC code CHIPIC to simulate the microwave generation. With the optimized structure, some typical results are obtained. A trapezoid voltage with a rise time of 1 ns and top value of 480 kV is used in the particle simulations, and the corresponding beam current is 42 kA. The impedance of the device is about 11.5 Ω.

Figure 6 shows the distribution of electrons in the particle simulation. From Fig. 6 we can see that the electrons emitted from the cathode are modulated well, forming 4 clear electronic spokes, which illustrates that the beam-wave interaction is sufficient.

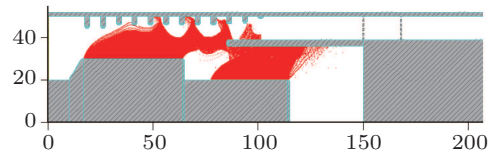


Fig. 6. (color online) Electron distribution in the particle simulation.

Figure 7 shows the plot of the output microwave power versus time. The microwave starts to grow at 5 ns and reaches a saturation value at 13 ns. The average microwave power is 1.5 GW, corresponding to an output power efficiency of 7.5%. The microwave frequency is fairly pure at 12.3 GHz as indicated in Fig. 8, which is consistent with our analyses of the dispersion curves illustrated in Section 2.

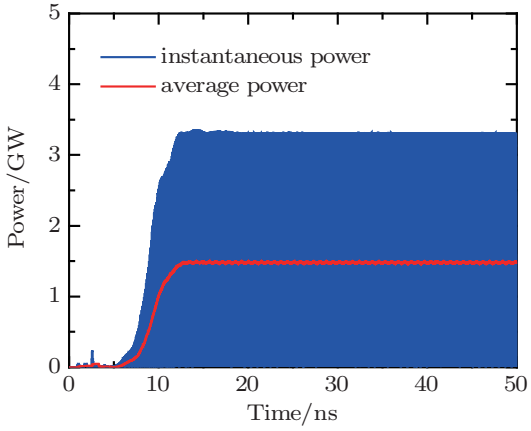


Fig. 7. (color online) Output microwave power versus time.

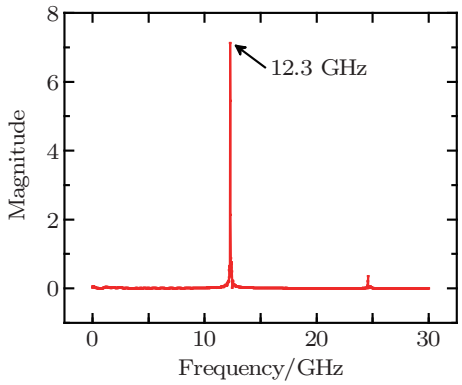


Fig. 8. (color online) Frequency spectrum of generated microwave.

Figure 9 shows the time frequency analysis of the produced microwave in the particle simulation. It can be seen that after the microwave achieves a saturation value at 13 ns, the power spectrum (doubled the electric field spectrum) becomes very stable at a frequency of 24.6 GHz in the microwave generation process.

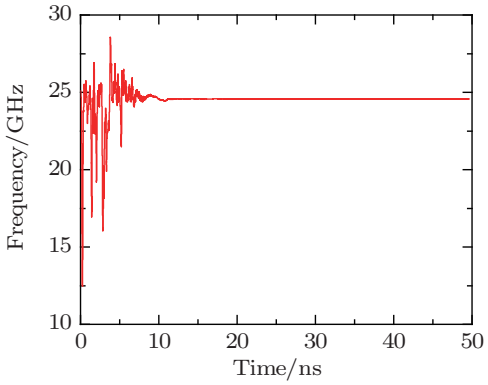


Fig. 9. (color online) Typical curve of the frequency versus time of the microwave in the simulation.

Figure 10 shows the distribution of the maximum axial electric field E_z in the SWS, calculated by CHIPIC when the device outputs 1.5-GW microwave power. From the figure, we can see that the maximum value is 1.2 MV/cm, while in the first Ku-band MILO designed by us, the maximum axial electric field is about 1.6 MV/cm under the same microwave output condition. Therefore, the power capacity of the improved Ku-band MILO is enhanced significantly and the risk of RF breakdown will be reduced greatly. This proves that the improvements we adopted are effective. It can also be seen from the figure that the distribution of E_z is the near π mode of TM01 mode because the phase difference of the adjacent cavities are 180°.

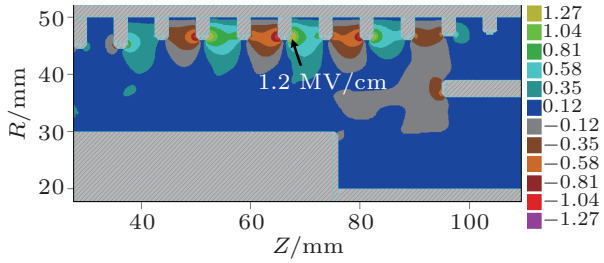


Fig. 10. (color online) Distribution of the maximal axial electric field E_z in the SWS.

5. Experimental investigation

The improved Ku-band MILO device is well assembled to a low impedance accelerator in our lab to conduct the experiments.

Figure 11 shows the typical diode voltage, current and the detector waveforms. It can be seen that the pulse voltage has a flat-top of around 500 kV. The rise-time, fall-time and the flat-top duration of the pulse voltage are about 50 ns, 40 ns, and 40 ns, respectively. The corresponding current at the flattop is measured to be 43 kA. The generated microwave is measured to have a power of 800 MW with a full width at half maximum (FWHM) pulse duration of 35 ns. The microwave waveform and the corresponding frequency spectrum are shown in Fig. 12. The center frequency is stabilized at pure 12.35 GHz, which is in accordance with the particle simulation frequency.

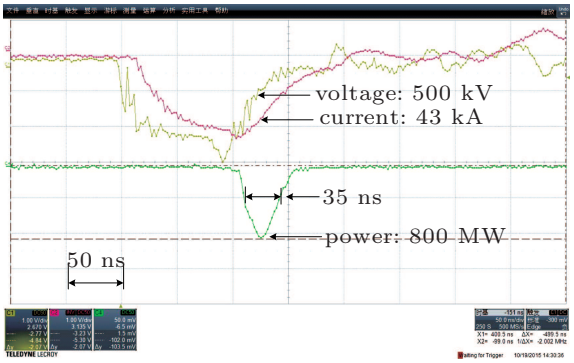


Fig. 11. (color online) Detection waveforms with diode voltage and beam current in experiment.

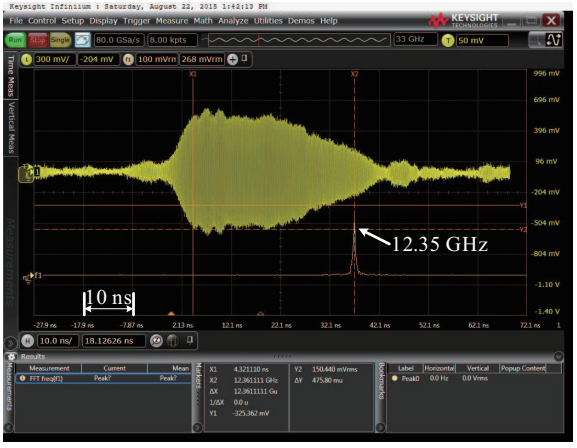


Fig. 12. (color online) Microwave waveform and its corresponding frequency spectrum.

Figure 13 shows the time-dependent frequency of the output microwave. It can be seen that the operating frequency has a good temporal stability in the microwave generation process. These experimental results show that the generated microwave has good single spectral characteristics.

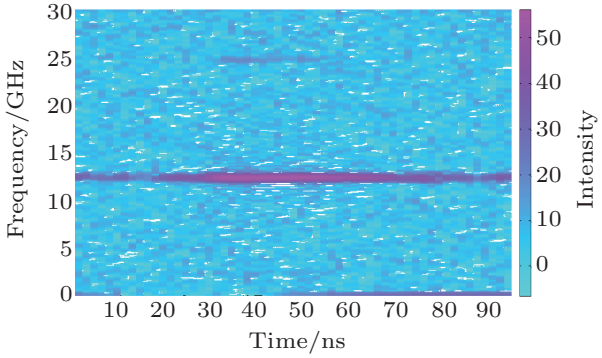


Fig. 13. (color online) Waveform of the time-dependent frequency of the microwave in experiment.

Finally, the far-field radiation pattern is measured. As can be seen from Fig. 14, the experimental far-field radiation pattern is consistent with the normalized theory far-field radiation pattern calculated by a three-dimensional (3D) electromagnetic simulation program. The good agreement suggests that the device operates in right mode (the π mode of TM01 mode).

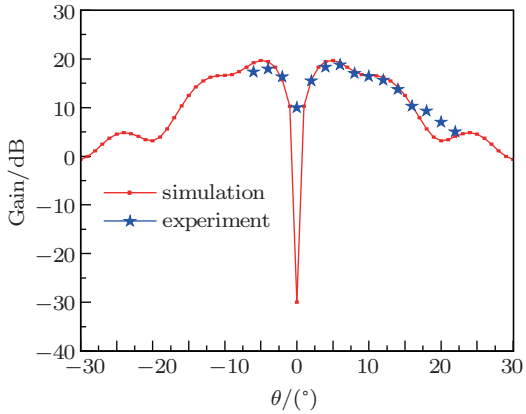


Fig. 14. (color online) Far-filed radiation patterns.

Compared with the experimental results of the first Ku-band MILO designed by us, the output power and the pulse width of the improved Ku-band MILO are enhanced greatly. The experimental results show that adopting the overmoded SWS really is conducible to the improvement of the power capacity of the Ku-band MILO. However, the output microwave power and the pulse width in experiments are both smaller than those in particle simulation. We think that the main reason is due to the drawback of the diode voltage waveform. As can be seen from the voltage waveform in Fig. 11, the rise-time and fall-time of the pulse voltage are too long (about 50 ns and 40 ns, respectively). This is disadvantageous for the operation of MILOs, especially for high-frequency MILOs, because MILOs almost do not produce microwave but emit large current in these two periods of time. It is easy to produce anode plasma due to the long-time bombardment of large current, which will result in reducing the output microwave power and shortening the microwave pulse width. Otherwise, there is a sharp peak in the fall-time of the diode voltage waveform, and the voltage jump is greater than 100 kV, which is not beneficial to the stable operation of MILO. Further efforts are being made to improve the output power and pulse width in experiment.

6. Conclusions

This paper presents the numerical and experimental investigation of an improved Ku-band MILO with overmoded SWS. The analyses of the dispersion relationship and the cold test indicate that the device can operate at the near π mode of the TM01 mode. The typical particle simulation results show that the improved Ku-band MILO generates the microwave with a power of 1.5 GW and frequency of 12.3 GHz under an input voltage of 480 kV and input current of 42 kA. In the experiment, a high power microwave with an average power of 800 MW, a frequency of 12.35 GHz, and pulse width of 35 ns is generated under a diode voltage of 500 kV and beam current of 43 kA.

References

[1] Barker R J and Schanmiloglu E 2001 *High Power Microwave Sources and Technologies* (New York: IEEE Press)
[2] Benford J and Swegle J A 1991 *High Power Microwaves* (Artech House, Norwood, MA)
[3] Lemke R W, Calico S E and Clark M C 1997 *IEEE Trans. Plasma Sci.* **25** 364
[4] Haworth M, Allen K, Baca G, Benford J, Englert T, Hackett K, Hendricks K, Henley D, Lemke R, Price D, Ralph D, Sena M, Shiffler D and Spencer T 1997 *Proc. SPIE* **3158** 28
[5] Eastwood J W, Hawkins K C and Hook M P 1998 *IEEE Trans. Plasma Sci.* **26** 698
[6] Lemke R W, Calico S E and Clark M C 1997 *IEEE Trans. Plasma Sci.* **25** 364
[7] Cousin R, Larour J and Gardelle J 2007 *IEEE Trans. Plasma Sci.* **35** 1467
[8] Zhang X P, Zhong H H and Yuan C W 2004 *High Power Laser Particle Beams* **15** 80
[9] Fan Y W, Yuan C W, Zhong H H, Shu T and Luo L 2007 *IEEE Trans. Plasma Sci.* **35** 379
[10] Fan Y W, Yuan C W and Zhong H H 2007 *IEEE Trans. Plasma Sci.* **35** 1075
[11] Li Z Q, Zhong H H and Shu T 2009 *Chin. Phys. Lett.* **26** 055201
[12] Li Z Q, Zhong H H and Shu T 2008 *High Power Laser Particle Beams* **20** 123
[13] Chen D B, Fan Z K and Zhou H J 2007 *High Power Laser Particle Beams* **19** 1352
[14] Fan Y W, Zhong H H, Li Z Q, Yuan C W, Shu T, Yang H W, Wang Y and Luo L 2011 *IEEE Trans. Plasma Sci.* **39** 540
[15] Ju J C, Fan Y W, Zhong H H and Shu T 2009 *Phys. Plasmas* **16** 073103
[16] Fan Y W, Zhong H H and Shu T 2008 *Chin. Phys. B* **17** 1804
[17] Fan Y W, Zhong H H and Yang H W 2008 *J. Appl. Phys.* **103** 123301
[18] Wen J, Tian Y C and Fan Z K 2011 *High Power Laser Particle Beams* **23** 3047
[19] Wen J, Chen D B, Wang D and Qin F 2013 *IEEE Trans. Plasma Sci.* **41** 2501
[20] Ling J P, Zhang J D, He J T and Jiang T 2014 *Phys. Plasmas* **21** 023114
[21] Ling J P, Zhang J D, He J T, Wang L and Deng B F 2014 *Rev. Sci. Instrum.* **85** 084702
[22] Zhang H, Shu T, Ju J C and Wu D P 2014 *Phys. Plasmas* **21** 033105
[23] Zhang H, Shu T, Ju J C and Wu D P 2014 *IEEE Trans. Plasma Sci.* **42** 6
[24] Zhang H, Shu T, Ju J C, Wu D P and Bai Z 2014 *Rev. Sci. Instrum.* **85** 084701
[25] Jiang T, Zhang J D, He J T, Ju J C, Li Z Q and Ling J P 2015 *IEEE Trans. Plasma Sci.* **43** 10
[26] Jiang T, Zhang J D, He J T, Li Z Q and Ling J P 2015 *Phys. Plasmas* **22** 102112
[27] Zhang D, Zhang J, Zhong H H and Jin Z X 2013 *Phys. Plasmas* **20** 073111
[28] Wu D P, Shu T, Zhu J, Zhang H and Ju J C 2014 *Phys. Plasmas* **21** 073105
[29] Zhang X P, Dang F C, Zhang J, Fan Y W and Li Z Q 2015 *Rev. Sci. Instrum.* **86** 024705
[30] Zhang X P, Zhong H H, Shu T, Yuan C W, Wang Y, Zhao Y S and Luo L 2005 *High Power Laser Particle Beams* **17** 1129
[31] Qin F, Wang D, Chen D B and Fan Z K 2009 *IEEE Trans. Plasma Sci.* **37** 10
[32] Pikunov V M and Chernyavskiy I A 2000 *Proc. SPIE* **4031** 286